# A Novel Cytoskeletal Structure Involved in Purse String Wound Closure and Cell Polarity Maintenance

**William M. Bement, Paul Forscher, and Mark S. Mooseker**

Department of Biology, Yale University, Kline Biology Tower, P.O. Box 6666, New Haven, Connecticut 06511-8112

***Abstract.*** The process of wound repair in monolayers of the intestinal epithelial cell line, Caco-$2_{BBe}$, was analyzed by a combination of time-lapse differential interference contrast (DIC) video and immunofluorescence microscopy, and laser scanning confocal immunofluorescence microscopy (LSCIM). DIC video analysis revealed that stab wounds made in Caco-$2_{BBe}$ monolayers healed by two distinct processes: (*a*) Extension of lamellipodia into the wounds; and (*b*) Purse string closure of the wound by distinct arcs or rings formed by cells bordering the wound. The arcs and rings which effected purse string closure appeared sharp and sheer in DIC, spanned between two and eight individual cells along the wound border, and contracted in a concerted fashion. Immunofluorescence analysis of the wounds demonstrated that the arcs and rings contained striking accumulations of actin filaments, myosin-II, villin, and tropomyosin. In contrast, arcs and rings contained no apparent enrichment of microtubules, brush border myosin-I immunogens, or myosin-V. LSCIM analysis confirmed the localization of actin filaments, myosin-II, villin, and tropomyosin in arcs and rings at wound borders. ZO-1 (a tight junction protein), also accumulated in arcs and rings around wounds, despite the fact that cell–cell contacts are absent at wound borders. Sucrase–isomaltase, an apically-localized integral membrane protein, maintained an apical localization in cells where arcs or rings were formed, but was found in lamellipodia extending into wounds in cells where arcs failed to form. Time-course, LSCIM quantification of actin, myosin II, and ZO-1 revealed that accumulation of these proteins within arcs and rings at the wound edge began within 5 minutes and peaked within 30–60 minutes of wounding. Actin filaments, myosin-II, and ZO-1 achieved 10-, 3-, and 4-fold enrichments, respectively, relative to cell edges which did not border wounds. The results demonstrate that wounded Caco-$2_{BBe}$ monolayers assemble a novel cytoskeletal structure at the borders of wounds. The results further suggest that this structure plays at least two roles in wound repair; first, mediation of concerted, purse string movement of cells into the area of the wound and second, maintenance of apical/basolateral polarity in cells which border the wound.

EPITHELIA are ubiquitous components of the metazoa, where they serve as selective barriers between tissues and the extracellular environment. Although epithelia are composed of individual cells, a single epithelial cell functions only within the context of its neighbors; isolated epithelial cells possess virtually none of the properties characteristics of an intact epithelium. For example, in the absence of neighboring cells, epithelial cells not only fail to act as barriers, for the simple reason that barrier functions are dependent on the formation of cell–cell junctions, but they are also relatively nonpolarized and do not express many proteins found in the same cells in mature monolayers (Louvard et al., 1992).

Just as individual epithelial cells function only within the context of the entire epithelium, so the functioning epithelium relies on the complete integrity of its constituents. Consequently, loss of cells from the epithelium either as a result of injury or normal cell turnover is disastrous for the epithelium and the organism unless it is quickly repaired. Given that intestinal epithelia are exposed to injury in a variety of pathological states (e.g., Feil et al., 1987) and are constantly extruding senescent cells from the villus tip (e.g., Madara, 1990), it is not surprising that mechanisms have evolved which effect rapid epithelial repair within the intestine (Feil et al., 1987; Moore et al., 1989; Madara, 1990). In fact, not only are large wounds repaired with incredible rapidity as assessed by microscopy and electrophysiological measurements (Feil et al., 1987), extrusion of senescent cells from the epithelium is accompanied by no detectable changes in permeability to macromolecules, suggesting that the monolayer suffers little or no lapse in barrier function during this process (Madara, 1990).

What mechanism underlies the remarkable resilience of epithelia? Studies of wound healing using isolated epithelia (Takeuchi, 1979; Radice, 1980; Takeuchi, 1983), and cultured epithelial cells (Gabbiani et al., 1978; Hergott et al.,

1989; McCormack et al., 1992; Nusrat et al., 1992), as well as numerous studies using endothelial cells (e.g., Selden and Schwartz, 1979; Gotlieb et al., 1981; Gordon et al., 1982; Gabbiani et al., 1983; Wong and Gottlieb, 1988; Gordon and Staley, 1990) and fibroblasts (e.g., Vasiliev et al., 1969), have led to the consensus that large wounds made in cell monolayers heal by extension of lamellipodia from cells bordering the wound onto the exposed substrate followed by migration of border cells into the wound itself. This process entails flattening of migrating cells and, presumably, temporary disruption of apical/basolateral polarity in those cells which close the wound.

We have reinvestigated the process of wound repair in a model system consisting of Caco-2 cells grown upon collagen-coated coverslips. Caco-2 cells are derived from a human colonic adenocarcinoma and will, when grown under appropriate conditions, differentiate into an intestinal enterocyte-like monolayer (Pinto et al., 1983). We have used a particular Caco-2 subclone, designated BBe, that was selected for its ability to differentiate in a manner that closely resembles its in vivo counterpart, particularly with respect to expression and distribution of cytoskeletal proteins (Peterson and Mooseker, 1992). Consistent with previous studies, we find that large wounds in Caco-$2_{BBe}$ monolayers heal by lamellipodial extension and cell migration. In contrast to large wounds, however, small wounds heal by purse-string contraction, apparently mediated by actomyosin-containing arcs and rings which form at wound borders and span multiple cells. That is, cells bordering small wounds function as a single unit, contracting in concert with each other to close wounds. The contractile arcs and rings that mediate wound closure also appear to restrict the diffusion of apically localized proteins such as sucrase–isomaltase, and the tight junction antigen, ZO-1, thereby maintaining cell polarity.

While this manuscript was in preparation, it was reported that wounds made in embryonic skin epidermis heal in the absence of lamellipodia formation (Martin and Lewis, 1992). It was observed that wounds closed smoothly in a purse string fashion, as if the entire wound border were subject to circumferential tension. It was further demonstrated that such wounds were surrounded by an actin cable, apparently continuous from cell to cell. The authors hypothesized that the actin cable effected wound healing by undergoing concerted contraction, thereby shrinking the wound perimeter (Martin and Lewis, 1992). The results of that study, conducted with avian embryos, and the present one, conducted using a cultured human cell line, suggest that purse string–driven cellular motility may represent a wide-spread biological phenomenon.

## Materials and Methods

### Cell Culture

The Caco-2 clone $C2_{BBe}$ (Peterson and Mooseker, 1992; referred to in that study as Caco-$2_{BBe1}$) was maintained at 37°C, 5% $CO_2$/95% air. Cells were cultured in 25 mM glucose DME (JRH Biosciences, Lenxa, KS), 10% FBS (Hyclone, Logan, UT), 2 mM glutamine (Sigma Immunochemicals, St. Louis, MO), 10 μg/ml transferrin (Boehringer-Mannheim Biochemicals, Indianapolis, IN), and penicillin/streptomycin/Fungizone (JRH Biosciences) as previously described (Peterson and Mooseker, 1992). For microscopy, cells were plated on acid-washed, collagen-coated coverslips, and then allowed to differentiate for 2–5 wk before wounding. Although Caco-$2_{BBe}$ cells grown under these conditions (i.e., on glass) do not reach the height achieved by Caco-$2_{BBe}$ cells grown on filters (5–10 μm on glass vs. 30–40 μm on filters; Peterson and Mooseker, 1992), they nevertheless form polarized monolayers, as assessed by immunofluorescence analysis.

### Wounding

Cells were wounded manually (i.e., by stabbing) with tungsten wire (.003 gauge; California Fine Wire Co., Grover City, CA) sharpened to a point by NaOH electrolysis. Due to the flexibility of the tungsten wire, stabbing frequently resulted in large wounds caused by the bowing and subsequent extension of the tungsten wire across the cell monolayers. Cell–cell adhesion is highly developed in Caco-$2_{BBe}$ cells, consequently, wounds made in this fashion frequently resulted in detachment of the cells surrounding the wound from the substrate, a condition which altered the manner in which wounds healed (see Results). As a means of mitigating this problem, wounds were made using sharpened tungsten wires wrapped around larger wire (18 awg-.82 $mm^2$; Belden Corporation, Chicago, IL), such that only the sharpened tip and several millimeters of the tungsten wire protruded beyond the end of the larger wire. This improved the reproducibility of wound size moderately, but it was still necessary to stab a given coverslip 60–80 times to produce one to three small (one to eight cell diameters, ~100 μm or less) wounds. The use of a micromanipulator did not significantly increase the frequency of small wounds, but did considerably slow the wounding process. Consequently, manual stabbing was used in all of the studies described below.

### Video Microscopy

After wounding, cells were mounted in a perfusion chamber, constructed as described previously (Forscher and Smith, 1988). Briefly, the coverslip with the wounded monolayer was overlain with a second coverslip, with two thin plastic strips, sealed to each coverslip with silicon grease, separating the two coverslips, thereby forming the chamber. The chamber was clamped into an aluminum holder machined to fit onto the Zeiss Axiovert-10 microscope stage (Carl Zeiss, Obekochen, Germany). The mounting process generally took between 15 and 30 mins, and locating a given wound generally took another 15 min, thus, time-lapse, differential interference contrast (DIC)[1] observations of wound healing usually commenced within 30–45 min after wounding. During observation, cells were perfused with media taken from the original dish into which coverslips were transferred; perfusion was such that the entire chamber contents were replaced every 10–15 min. Stage temperature was maintained at 34°C using a Dage air curtain (Dage-MTI Inc., Michigan City, MI). Time-lapse, DIC analysis, and image processing were conducted as described by Forscher and Smith (1988).

### Immunofluorescence

Two similar protocols were used for immunofluorescence, depending on whether cells were wounded and analyzed by time-lapse video microscopy, or wounded and processed directly for confocal laser-scanning microscopy. In the first case, cells were prepared by sequentially perfusing the observation chamber with the following solutions (room temperature unless otherwise indicated): (*a*) two washes in PBS; (*b*) 15-min fixation in ice-cold 4% paraformaldehyde in PBS/50 mm EGTA ("MB" medium); (*c*) 5-min permeabilization in 4% paraformaldehyde and 1% Tx-100 in MB; (*d*) five washes in 0.1% Tx-100 + 1% BSA (Sigma Immunochemicals) in MB; (*e*) 15 min in 10% BSA in MB; (*f*) 1 h in MB + 120 nM rhodamine phalloidin (Molecular Probes, Eugene, OR) and primary antibody (for primary antibodies, see below); (*g*) 20 washes in MB + 0.1% Tx-100; (*h*) 1 h in 10 μg/ml of FITC-conjugated anti-rabbit or anti-mouse IgG (Jackson Immunological Research Labs, West Grove, PA) in MB; (*i*) 20 washes in MB + 0.1% Tx-100; and (*j*) mounting in 20 mM *N*-propyl-galate in PBS/80% glycerol. Fluorescence images were obtained as described by Forscher and Smith (1988). The primary antibodies used were as follows: anti-human platelet myosin-II (Biomedical Technologies Inc., Stoughton, MA); HPLC-purified anti-chicken brush border myosin-I (CX-1 from Carboni et al., 1988; note that CX-1 recognizes three putative myosins I in Caco-$2_{BBe}$ cells [Peterson and Mooseker, 1992], hence, in the Results we refer to staining of CX-1 im-

1. *Abbreviations used in this paper*: DIC, differential interference contrast; LSCIM, laser scanning confocal immunofluorescence microscopy.

munogens); affinity-purified anti-chicken myosin-V (Espreafico et al., 1992); anti-chicken fodrin serum (Harris et al., 1986; a lavish gift from Dr. Jon Morrow, Yale University); affinity-purified anti-chicken villin (West et al., 1988); anti-rat sucrase-isomaltase serum (Quaroni, 1986; a munificent gift from Dr. Andrea Quaroni, Cornell University, Ithaca, NY); anti-human erythrocyte tropomyosin (an extravagant gift from Dr. Velia Fowler, Scripps Clinic, La Jolla, CA); anti-rat β-tubulin (Sigma Immunochemicals); affinity-purified anti-Z0-1 peptide (Willot et al., 1992; a princely gift from Dr. Jim Anderson, Yale University, New Haven, CT).

All of the antibodies used in this study recognize the proteins against which they were raised as determined by Western blotting of Caco-$2_{BBe}$ extracts (Peterson and Mooseker, 1992; W.M. Bement, unpublished results) and by specific immunofluorescence staining of the appropriate structures in unwounded Caco-$2_{BBe}$ monolayers (e.g., CX-1 specifically stains microvilli; Peterson and Mooseker, 1992; anti-human erythroid tropomyosin specifically stains stress fibers; W. M. Bement, unpublished results).

### *Laser Scanning Confocal Immunofluorescence Microscopy*

For confocal microscopy, coverslip-grown monolayers in six-well culture plates were wounded, allowed to heal 5 min-3 h as described in the Results, and then processed in six-well plates in the following manner (room temperature unless otherwise indicated): (*a*) two washes in PBS; (*b*) 15-min fixation in ice-cold 4% paraformaldehyde in PBS/50 mM EGTA ("MB" medium); (*c*) 5-min permeabilization in 4% paraformaldehyde and 1% Tx-100 in MB; (*d*) 3× 10-min washes in 0.1% Tx-100 + 1% BSA; (Sigma Immunochemicals) in MB with gentle rotation; (*e*) 45 min in 10% BSA in MB; (*f*) 1 h at 37°C in MB + 120 nM rhodamine phalloidin and primary antibody; (*g*) 3× 10-min washes in MB + 0.1% Tx-100 with gentle rotation; (*h*) 1 h at 37°C in secondary antibody; (*i*) 3× 10-min washes in MB + 0.1% Tx-100 with gentle rotation; (*j*) mounting in 20 mM *N*-propyl-galate in PBS/80% glycerol.

After processing as described above, wounded monolayers were analyzed on a laser-scanning, confocal microscope (Bio-Rad Laboratories, Cambridge, MA) as previously described (Peterson and Mooseker, 1992). Laser Scanning Confocal Immunofluorescence Microscopy (LSCIM) analysis with the Bio-Rad microscope allowed simultaneous analysis of two different fluorophores within the same focal plane, consequently, the microscope output yielded split-screen, double-label images showing either en face or computer-generated cross-sectional views of actin filaments and the other proteins as described in the Results. This type of analysis allowed unambiguous determination of the presence or absence of a given protein within the focal plane of the actin filament cables.

### *LSCIM Quantification of Fluorescence Intensity*

To obtain semi-quantitative information with respect to the apparent localization of actin filaments, myosin-II, and Z0-1 at wound borders, fluorescence intensity was measured within a 10 × 10 pixel square on the monitor using the Bio-Rad software. Signal intensities measured within arcs and rings were normalized by dividing the fluorescence intensity for actin filaments, myosin-II, or Z0-1 within arcs or rings along wound borders by the most intense fluorescence signal within the same cell, but on a cell edge distal to the wound. Optical sectioning was necessary to determine the most intense control (nonwound) signal since the brightest signals distal to the wound edge were often above the focal plane of the brightest signals at the wound edge. While this method undoubtedly underestimates the relative fluorescent intensities within arcs and rings, it avoids potential artifacts due to differential expression/detection of given proteins within different cells.

## *Results*

### *Wound Healing in Living Cell Monolayers*

To analyze the process of wound healing in living Caco-$2_{BBe}$ monolayers, cells were plated on collagen-coated coverslips, and then, 2-5 wk after achieving confluence, monolayers were stabbed manually with sharpened tungsten wires and observed by time-lapse, DIC video microscopy as described

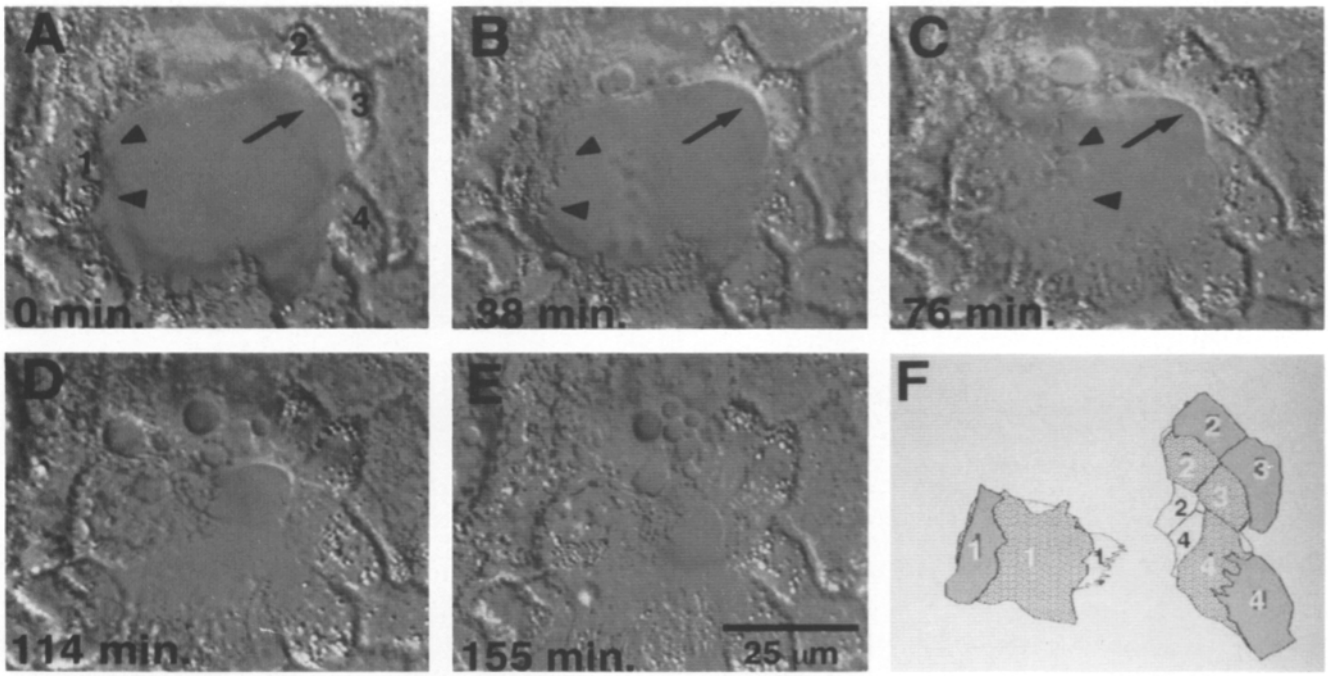


*Figure 1.* Time-lapse, DIC analysis of a wound healing by both lamellipodial extension and purse string contraction. (*A–E*) DIC images showing lamellipodia extending into wound (*arrowheads*) and cells moving into wound via purse string contraction (*arrows*). Minutes indicate the time elapsed from the beginning of observation. Edges of cells moving by purse string contraction (*arrows*) appear sharp and sheer. (*F*) Outline tracings of cells 1–4 in *A* at 0 min (*gray*), 80 min (*light gray*), and 155 min (*white*). 0 min outline shows the whole cell, subsequent tracings show the edges bordering the wound. Note the broadening of free borders of cells moving via lamellipodial extension (cells *1* and *4*) and shortening of free borders moving via purse string contraction (cells *2* and *3*); cell *3* is actually "squeezed" out of wound edge by cells *2* and *4*.

in Materials and Methods. Wounds were observed to close via two distinct processes, both of which are evident in Fig. 1. The first process, previously documented in other studies, involved extension of lamellipodia by cells bordering the wound onto the exposed substrate of the wound and migration of border cells into the wound (Fig. 1, *arrowheads*). The second process entailed a smooth, "purse string" like shrinkage of the wound border, wherein cells bordering the wound moved into the wounded area in the absence of lamellipodial extension (Fig. 1, *arrows*; also see below). The wound edges of those cells involved in purse string closure appeared characteristically sharp and sheer in DIC from the apical cell boundary to the substrate (Fig. 1, *arrows*). The manner of wound closure varied considerably from wound to wound, with some wounds healing entirely by lamellipodial extension (not shown), some entirely by purse string contraction (see below), and some by both mechanisms (Fig. 1). Generally, large wounds (>8 cell diameters; >100 μm), or wounds in which cell–cell contacts were disrupted tended to heal by lamellipodial extension, whereas smaller wounds (<8 cell diameters) tended to heal by purse string closure.

Purse string wound closure appeared to involve the concerted contraction of cell edges at the boundary of wounds. To better visualize this process, the outline of cells bordering the wound were traced from the DIC images such that cell shape could be more easily visualized. As shown in Fig. 1 *F*, the free edges (i.e., those which border wounds) of cells which moved into the wound via extension of lamellipodia became much larger as healing commenced. In contrast, as the two cells in the upper right portion of the wound moved into the wound, the length of their free edges shortened concurrent with their translocation into the wound, supporting the impression that purse string wound closure is mediated by concerted contraction of cell edges at the wound border.

### *Actin and Myosin II Are Concentrated in Arcs and Rings at Wound-Borders*

The purse string wound closure described above suggested the involvement of a contractile network in the process of wound healing. To investigate this possibility, wound closure was monitored by time-lapse DIC followed by correlative immunofluorescence. After documenting purse string closure with video analysis, cells under observation were fixed, permeabilized, and stained with rhodamine phalloidin alone or rhodamine phalloidin and anti-myosin II antibodies followed by FITC-conjugated secondary antibodies. Wound borders undergoing purse string contraction (Figs. 2, *A–E*; and 3, *A–C*) displayed a striking concentration of filamentous actin (Figs. 2 *F*, *arrows*; and 3 *D*) and myosin-II (Fig. 3 *E*). DIC analysis and rhodamine phalloidin staining confirmed that few (Fig. 2 *F*, *arrowheads*) or no (Fig. 3 *F*) lamellipodia formed in these wounds. Fig. 3 reveals two other important points: first, the contractile ring formed well above the substrate and closed farther than lamellipodial extension at the substrate (compare Fig. 3, *D–F*) such that the

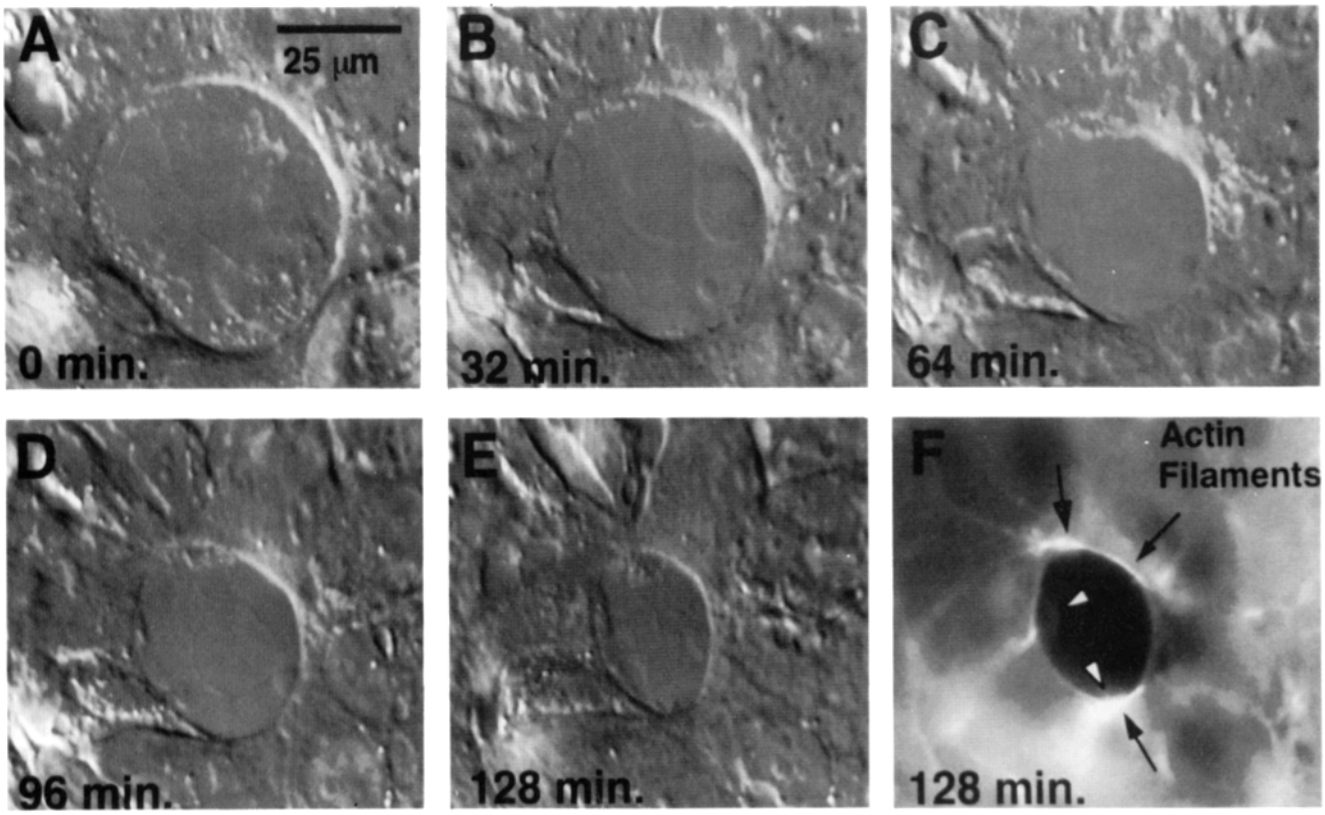


*Figure 2.* Time-lapse, DIC analysis of wound closure followed by correlative fluorescence analysis of actin filament distribution. (*A–E*) DIC documentation of purse string wound closure. Minutes indicate the time elapsed from the beginning of observation. (*F*) Rhodamine phalloidin staining following fixation of the wound shown in *E*, demonstrating a concentration of filamentous actin along the wound borders (*arrows*). Two small lamellipodia are visible in the wound (*F*, *arrowheads*).

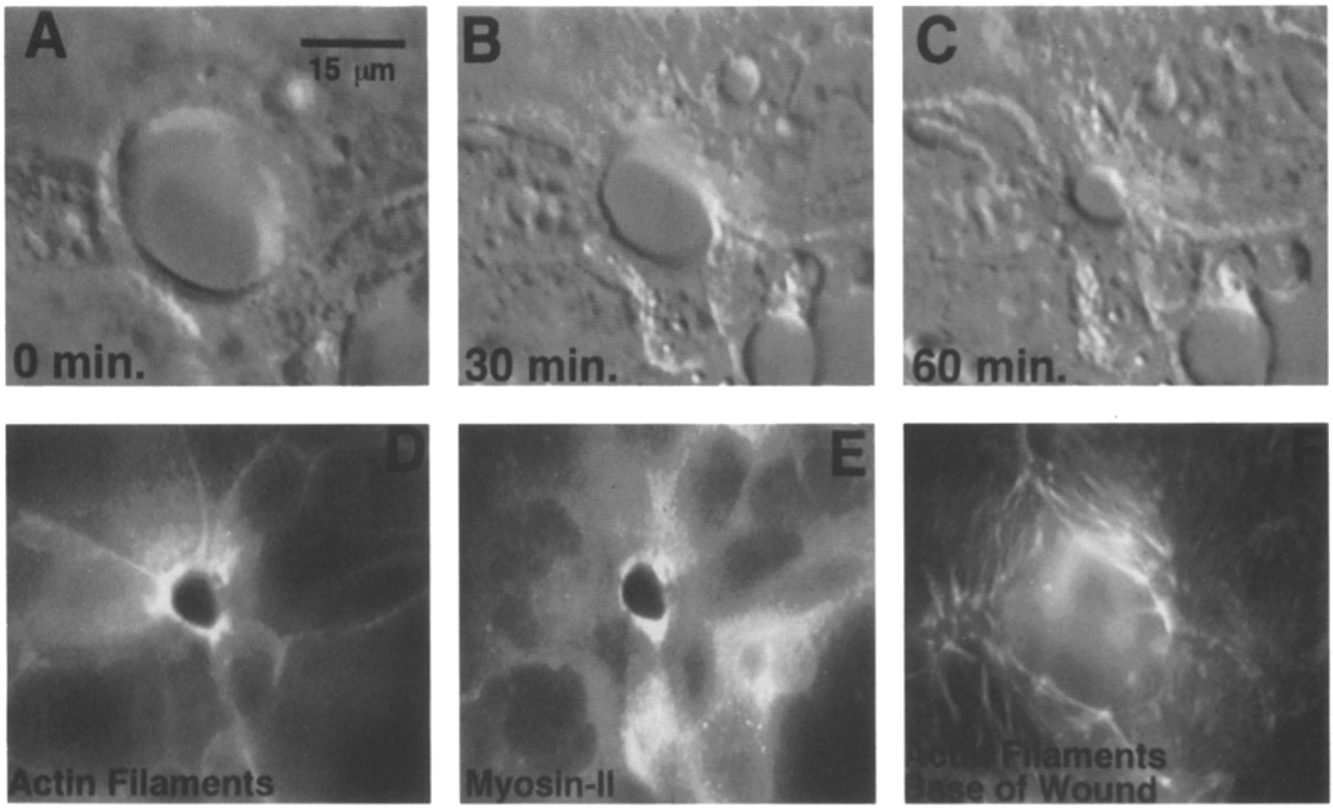


*Figure 3.* Time-lapse DIC analysis of wound closure followed by correlative immunofluorescence of actin filament and myosin-II distribution (*A–C*) DIC images of wound closure, ~3 μm above the substrate; minutes indicate the time elapsed from the beginning of observation. (*D*) Rhodamine phalloidin staining following fixation of the wound shown in *C*, demonstrating the concentration of actin filaments in the same focal plane observed in *A–C* to undergo purse string contraction. (*E*) Myosin-II colocalization along wound borders in the same focal plane as the actin ring observed in *D*. (*F*) Rhodamine phalloidin staining at the substrate focal plane of the wound in *C–E*, showing that the wounded substrate has not yet been covered by lamellipodia.

wound assumed a conical shape (i.e., narrow at the top and broad at the base); second, the apical localization of actin filaments and myosin clearly coincides with the apical purse string closure observed by DIC (compare Fig. 3, *C* and *E*). The amount of time required for wound healing varied considerably from wound to wound, depending on wound size, mode of healing, etc. For example, based on their closure rates before fixation, the wounds shown in Figs. 2 and 3 would be predicted to close in 4.8 and 1.5 h, respectively.

Large wounds typically failed to form continuous actomyosin rings around their perimeters, however, they often formed actomyosin arcs which spanned several cells along the wound border (Fig. 4, *A–C*, *arrows*). High magnification views confirmed the cablelike nature of such arcs (Fig. 4 *E*, *arrows*) and also showed that microvilli were largely absent below the focal planes of actomyosin cables (Fig. 4 *E*, *arrowheads*), while numerous microvilli were present in areas apical to the cables (Fig. 4 *D*, *arrowheads*).

### *LSCIM Analysis of Cytoskeletal Proteins at Wound Borders*

To confirm the apparent concentration of actin and myosin II in contractile arcs and rings, and to extend the investigation to other proteins known to comprise the cytoskeleton of intestinal epithelial cells, cell monolayers were wounded, allowed to heal for 30 min to 3 h, and then analyzed by LSCIM. Optical sectioning demonstrated that both myosin-II and filamentous actin were localized within discrete focal planes in arcs and rings at the edges of wounds (Fig. 5, *A* and *B*, *arrows*), with fluorescent intensities greatly exceeding intensities in areas distal to the wound (not shown, but see below). As seen above (Fig. 4 *B*), such arcs and rings were clearly continuous from cell to cell along the wound border (Fig. 5 *B*). To obtain cross-sectional views of the contractile apparatus, X–Z series through arcs and rings were generated and digitally converted to lateral cross-sections. In lateral views of arcs and rings, both actin filaments and myosin-II often appeared as discrete, bright points above the level of the substrate (Figs. 5, *C* and *D*), consistent with the apparent cablelike localization seen in en face views. Control staining with nonspecific rabbit IgGs (Fig. 5 *E*) followed by FITC-conjugated anti-rabbit secondary antibodies in conjunction with rhodamine phalloidin showed no FITC staining of wound borders, confirming both the specificity of the primary antibody and demonstrating that the observed myosin-II signal was not a result of "bleed through" from the relatively strong rhodamine phalloidin signal (Fig. 5 *F*). As a second control to ensure that the observed localization of actin filaments and myosin-II around wounds did not represent artifactual increases in fluorescence intensity due to increased access of rhodamine-phalloidin or antibodies to

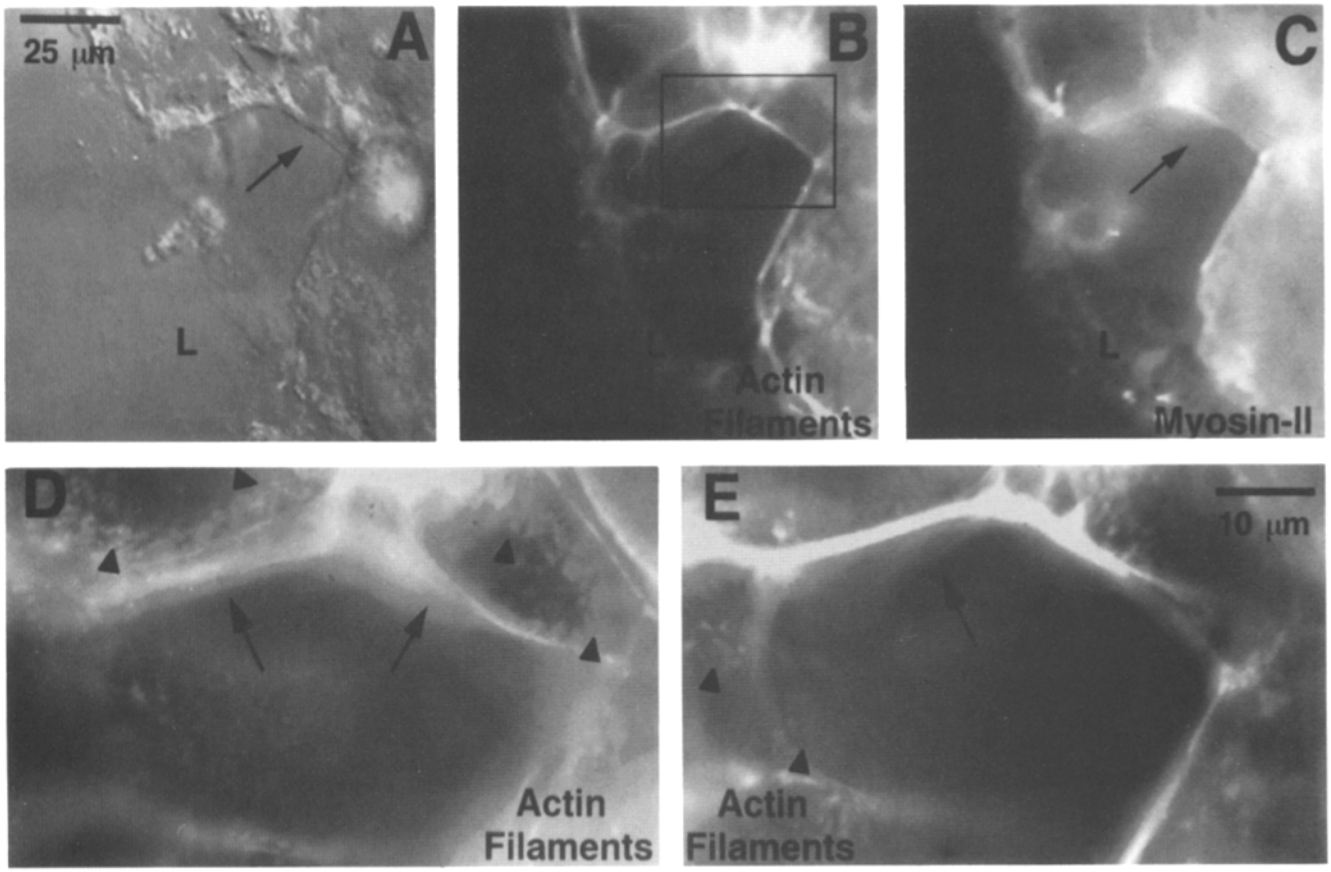


*Figure 4.* DIC/immunofluorescence views of actomyosin arcs at the border of a large, 5.5 h wound. (*A*) DIC image showing the sharp, sheer edge above a lamellipodia (*L*) at the wound (*W*) border. (*B*) Rhodamine phalloidin stain showing actin filament cables (*arrows*) and lamellipodia (*L*) in the wound shown in *A*. (*C*) Myosin-II stain of the same portion of the wound shown in *B*. Note the obvious coincidence of actin filaments in *B* and myosin-II in *C* (*arrows*). (*D*) High magnification of the boxed area shown in *B*, just above the focal plane of the cable (*arrows*). Note the presence of numerous microvilli (*arrowheads*) above the cable. (*E*) High magnification view of the boxed area shown in *B* just below the focal shown in *D*. Note the obvious, cablelike appearance of the actomyosin arc (*arrows*) and the relative paucity of microvilli (*arrowheads*).

wound sites, monolayers were wounded after fixation, but before incubation in rhodamine–phalloidin and 1° antibody. Monolayers processed in this fashion showed no apparent localization of either actin filaments or myosin II around wounds (Fig. 5, *G* and *H*).

The distributions of villin, an actin filament–bundling/severing protein normally localized to microvilli, and tropomyosin, an actin filament binding protein normally localized to stress fibers and the terminal web, were also analyzed by LSCIM. Villin showed a striking localization around wound borders (Fig. 6 *A*), but not confined precisely within actin cables (Fig. 6 *B*, *arrows*). Rather, villin appeared concentrated around the entire area of the wound, at the apparent expense of its normal localization within microvilli, which, within cells immediately bordering the wound, was comparatively slight (Fig. 5 *A*, *arrowheads*). Tropomyosin, like myosin-II, colocalized with actin filaments in multicellular cables which circumscribed wounds (Fig. 6, *C* and *D*, *arrows*).

The distribution of several other known cytoskeletal constituents of Caco-$2_{BBe}$ cells, including fodrin and brush border myosin-I, was also analyzed by LSCIM. Fodrin showed a modest, patchlike colocalization with actin arcs and rings (Fig. 7, *A* and *B*). Similar to figures above (e.g., Figs. 1 *E* and 5, *A* and *B*), Fig. 7 *B* also demonstrates that the actin filament arcs and rings can coexist not only in the same wound, but also in the same cell as lamellipodia. The distribution of brush border myosin-I in wounds was followed using the mAb, CX-1 (Carboni et al., 1988). CX-1 immunogens are localized in the microvilli of Caco-$2_{BBe}$ cells (not shown but see Peterson and Mooseker, 1992), but show no apparent colocalization with actin filaments in arcs and rings around wound borders (Fig. 7, *C* and *D*).

Neither microtubules nor myosin-V (not shown) showed localizations within actomyosin cables around wound borders. While microtubule staining did reveal numerous cells (~5%) with mitotic figures, these were in no obvious orientation with respect to the wounds. Moreover, given the rapidity of the wound-healing response (1.5–5 h; and see above) and the slowness of the mammalian cell cycle (~24 h), it is unlikely that cell division drives the observed purse string wound healing.

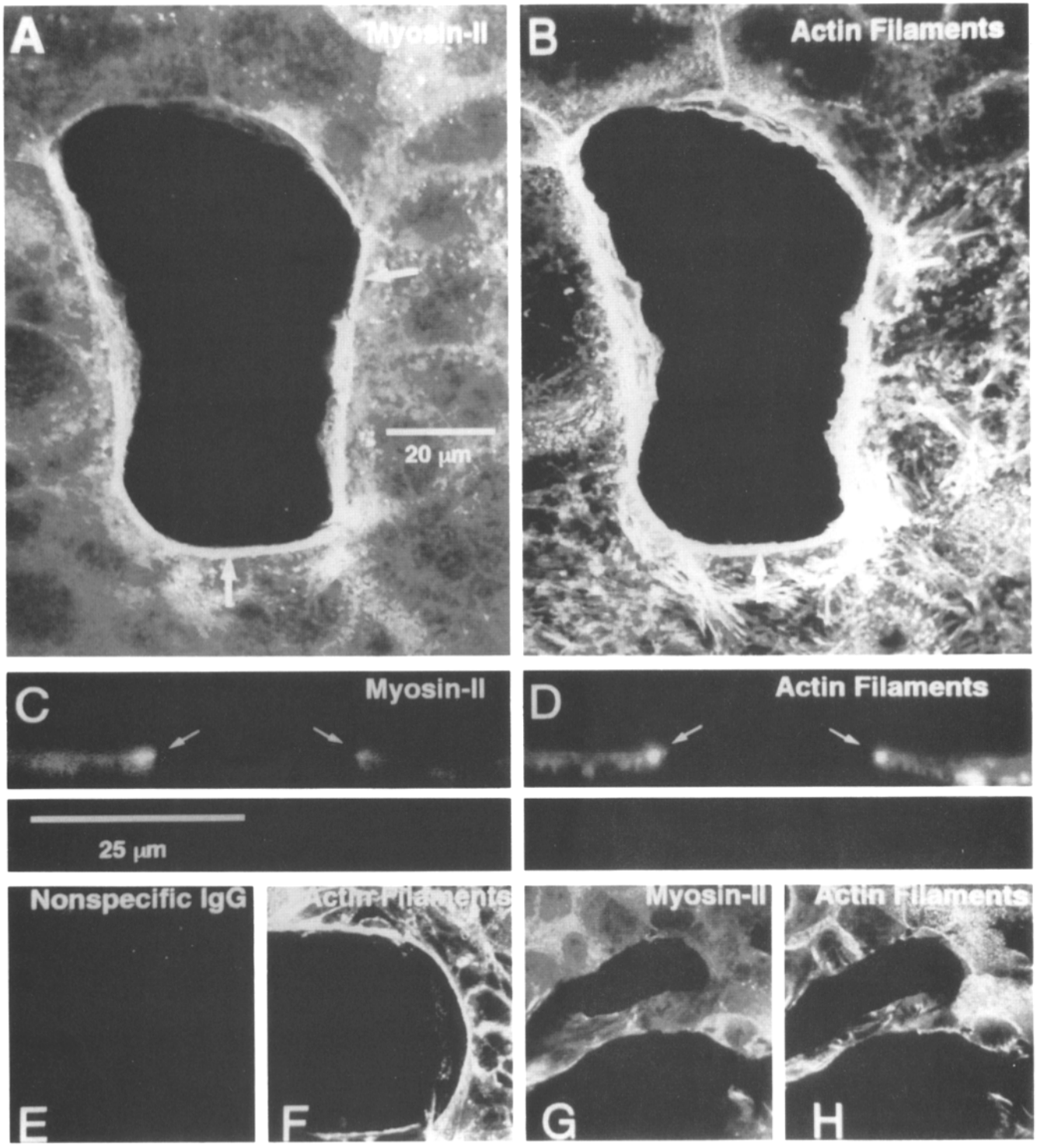


*Figure 5.* LSCIM images of the distribution of actin filaments, myosin-II, and control IgGs in wounds made before (*A–F*) and after (*G* and *H*) fixation. (*A* and *B*) Same-plane, en face view of the colocalization of actin filaments and myosin-II in arcs (*arrows*) at the border of a wound (*black area*), at and slightly above the plane of the substrate. (*C* and *D*) Computer generated, cross-section of a 1 h wound showing colocalization of myosin-II and actin filaments in bright, discrete dots (*arrows*) at the wound border, above the level of the substrate (*thin white line*). (*E* and *F*) Same-plane, en face view of wound showing lack of control rabbit IgG staining (*E*) even in the presence of a strong rhodamine phalloidin signal (*F*). (*G* and *H*) Same-plane, en face view of a wound made after fixation but before incubation in rhodamine phalloidin and antimyosin-II. Neither myosin-II (*G*), nor filamentous actin (*H*) show any localization at wound borders (*black areas*).

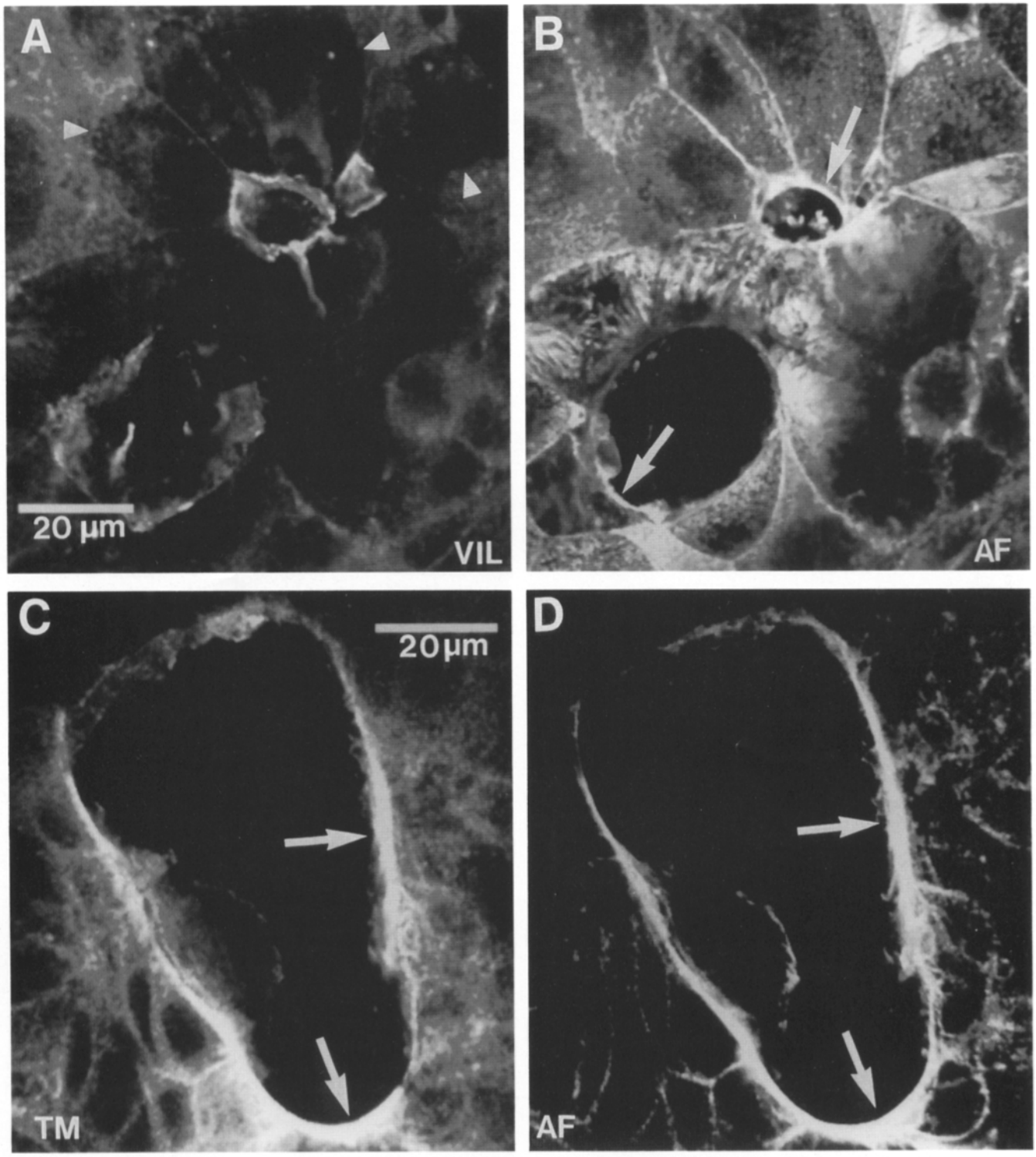


*Figure 6.* LSCIM images of villin, tropomyosin, and actin filaments in a 3 h wound. (*A* and *B*) Same-plane, en face view of villin (*A*) in and around the actin rings (*B*) which encircle the wound (*arrows*). Villin staining is comparatively weak in the microvilli of cells bordering the wound (*arrowheads*). (*C* and *D*) Same-plane, en face view of tropomyosin (*C*) and actin filaments (*D*) showing that both are concentrated in arcs around wound edges (*arrows*).

### *Maintenance of Apical/Basolateral Polarity at Wound Edges*

The observation that microvilli were numerous above (i.e., apical to) but not below (i.e., basal to) actomyosin cables at wound borders suggested that actomyosin cables might act to restrict the diffusion of apical structures and proteins to the basolateral domain along free cell edges. To further investigate this possibility, the distribution of ZO-1 and sucrase–isomaltase following wounding were analyzed by LSCIM.

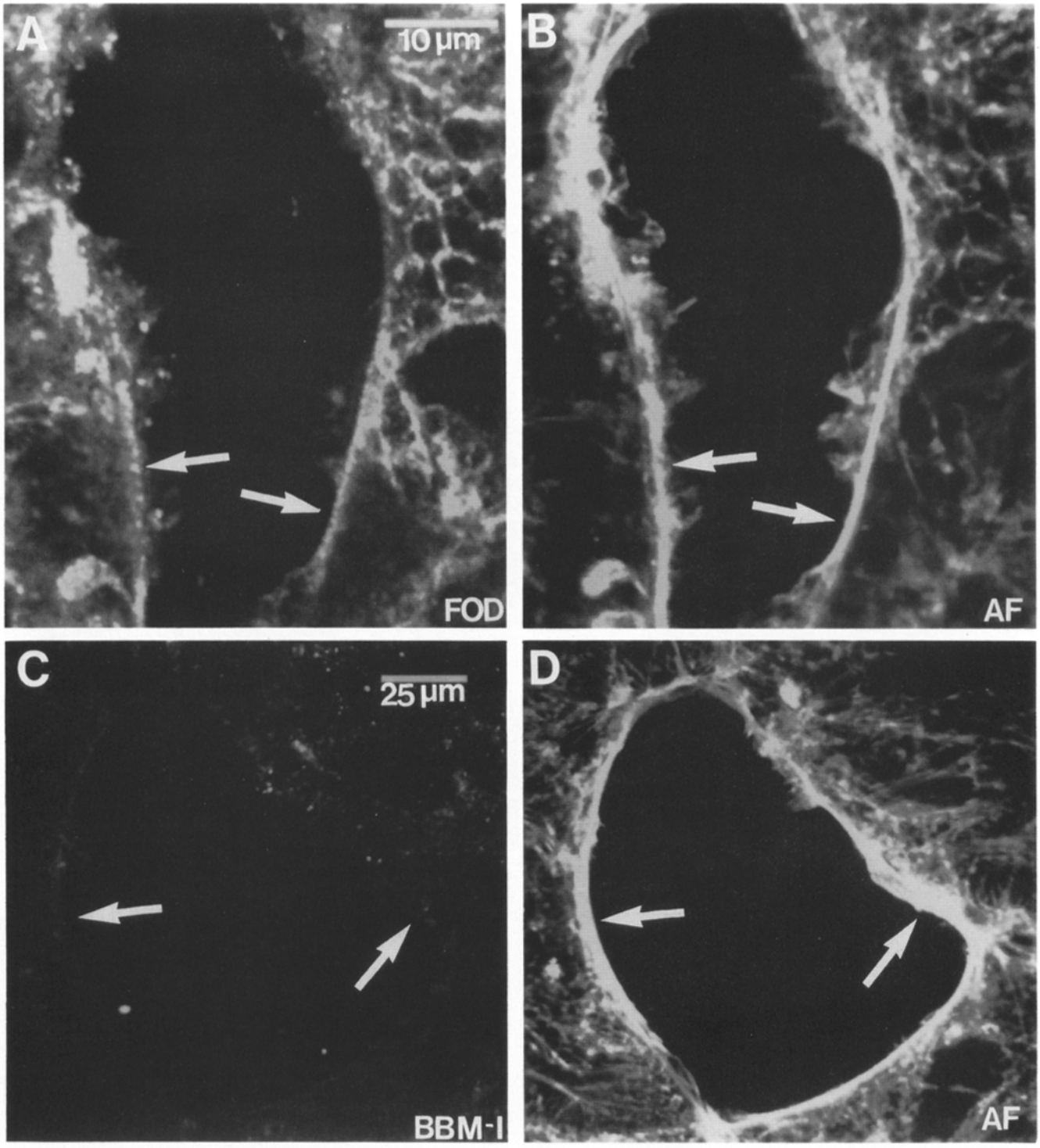


*Figure 7.* LSCIM images of fodrin, brush border myosin-I, and actin filament distribution around 3 h wounds. (*A* and *B*) Same plane, en face view showing colocalization of fodrin patches (*A*, *arrows*) with actin cables (*B*, *arrows*) encircling the wound. (*C* and *D*) Same-plane, en face view showing brush border myosin-I (*C*) and actin filament (*D*) distribution around wound. There is no apparent colocalization of CX-1 immunogens with the actin filament ring (*arrows*) encircling the wound.

Z0-1 is a component of tight junctions (Anderson and Stevenson, 1992), and, in unwounded Caco-$2_{BBe}$ monolayers, is localized at the boundary between the apical and the basolateral domains (Peterson and Mooseker, 1992). LSCIM analysis demonstrated that Z0-1 not only remained above the substrate in cells where actin arcs and rings were formed as seen in both en face (Fig. 8, *A* and *B*, *arrows*) and lateral (Fig. 8, *C* and *D*) sections, but actually appeared more concentrated along the free edges of wounds than in areas distal to wounds (Fig. 8 *A*).

Sucrase–isomaltase, an apically-localized, integral membrane protein (e.g., Quaroni, 1986), is expressed in only a

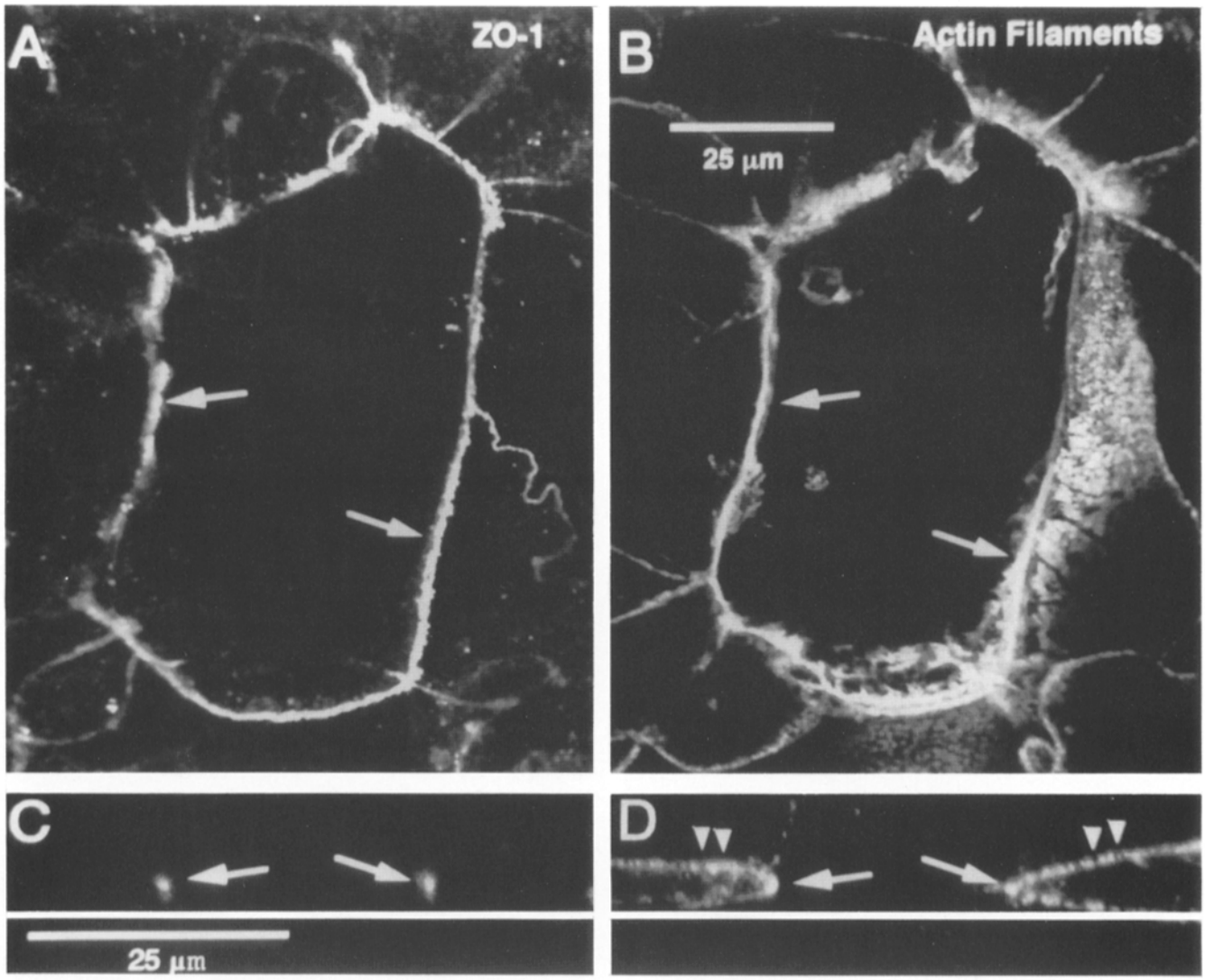


*Figure 8.* LSCIM images of ZO-1 and actin filaments around a 1 h wound. (*A* and *B*) Same-plane, en face view showing colocalization of ZO-1 (*A*) and actin filaments (*B*) in arcs around the wound (*W*). (*C* and *D*) Lateral view of a 1 h wound showing colocalization of ZO-1 (*C*) and actin filaments (*D*) in intense dots (*arrows*) above the substrate (*thin white line*). Double arrowheads denote rhodamine phalloidin staining of the brush border microvilli.

subset of Caco-$2_{BBe}$ cells, so that en face staining for sucrase–isomaltase reveals a "patchwork quilt" pattern of immunofluorescence (Peterson and Mooseker, 1992). Consequently, many wounds had to be examined in order to find cells that both formed actin cables at their borders and expressed high concentrations of sucrase–isomaltase. In cells which satisfied both criteria, sucrase–isomaltase was excluded from lamellipodia (i.e., it remained apical to the substrate) as seen in both en face images (Fig. 9, *A* and *B*, *arrowheads*) and in cross-section (Fig. 9, *A* and *B*, *insets*, *arrowheads*). In contrast, in cells bordering wounds which failed to form actin cables, sucrase–isomaltase could be seen in lamellipodia (i.e., it did not remain apical to the substrate; Fig. 9, *C* and *D*, *arrowheads*).

The apparently high concentration of actin filaments, myosin-II, and Z0-1 at wound borders suggested that their presence in arcs and rings did not merely represent remnants of localizations that existed before wounding. To assess this possibility, a time course, LSCIM analysis of fluorescence intensity was conducted for actin filaments, myosin-II, and Z0-1. The signal intensity relative to nonwound edges of the same cells was quantified as described in the Materials and Methods at 5 min, 30 min, 1 h, and 3 h after wounding using wounds less than eight cell diameters in size. An increase in relative concentration of actin filaments in arcs and cables at wound borders began within 5 min and peaked at 1 h (Fig. 10). Myosin-II and Z0-1 also showed increases in relative concentrations within 5 min of wounding and reached a plateau within 30 min. Actin filaments, myosin-II, and Z0-1 achieved 5.0, 3.4, and 2.2-fold enrichments, respectively, relative to nonwound edges within the same cells (Fig. 10). It is important to note, however, that the signals at wound edges represent the fluorescence output from a single cell, whereas control (nonwound) signals are derived from the output of two cells. Thus, the estimates for the relative concentrations of actin filaments and Z0-1, which are both tightly localized

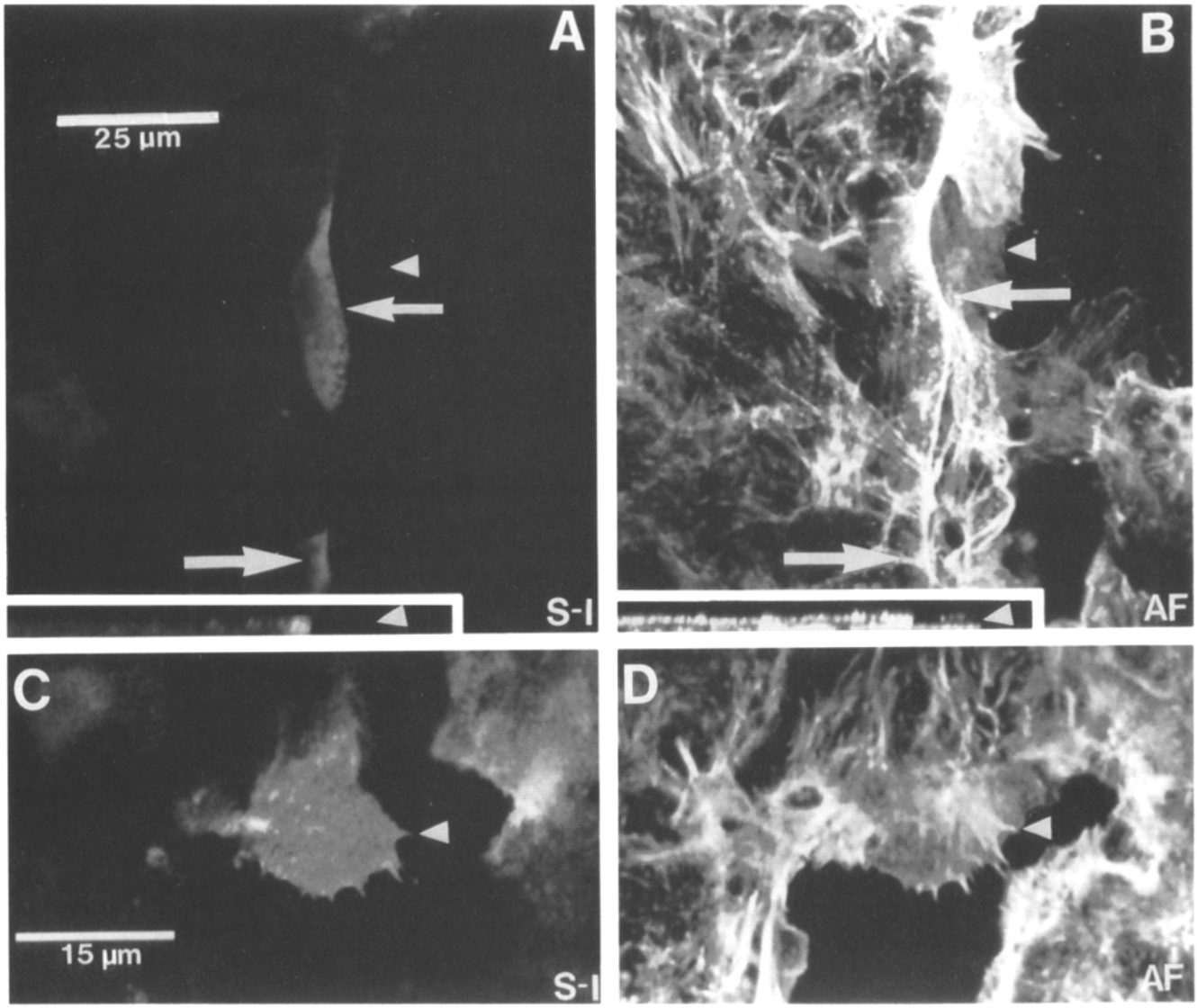


*Figure 9.* LSCIM images of sucrase-isomaltase and actin filaments around a 3 h wound. (*A* and *B*) Same-plane, en face view showing that sucrase isomaltase (*A, arrows*) is found at or above an actin cable (*B, arrows*) at the wound border, but not in a lamellipodium in the same cell (*A* and *B, arrowheads*). (*Insets*) Lateral views of the same wound confirm that sucrase-isomaltase (*A, arrow*) is excluded from the lamellipodium (*A* and *B, arrowheads*) below the actin cable (*B, arrow*). (*D* and *E*) Same-plane, en face view showing that sucrase-isomaltase (*C, arrowhead*) is not excluded from lamellipodia (*D, arrowhead*) in cells where actin cables fail to form.

to cell boundaries in Caco-$2_{BBe}$ cells, should properly be doubled, to 10 and 4.4, respectively.

## *Discussion*

The results of this study indicate that wounded monolayers of Caco-$2_{BBe}$ cells assemble a specialized cytoskeletal structure around the edge of wounds which contains filamentous actin, myosin-II, villin, tropomyosin, and the tight junction protein, ZO-1. However, two other potential explanations of these results must also be considered. First, because the apparent concentration of the various cytoskeletal proteins occurs at the border of the wound, it is possible that the observed phenomenon merely represents an "edge effect," a result of out-of-focus information increasing the fluorescence signal at the wound margin. This possibility is excluded by the confocal microscopic analysis which clearly showed that the localized cytoskeletal proteins were generally concentrated within a single optical plane when viewed en face or as a single bright point when viewed in cross section. Second, the apparent concentration of cytoskeletal antigens at the wound border could result from increased accessibility of cytoskeletal antigens to their respective antibodies relative to those antigens distal from the wound site. This possibility is excluded by the fact that at least three of the proteins in question, actin, conventional myosin, and ZO-1, show an increase in concentration at the wound margin at increasing time intervals following wounding and by the fact that no apparent accumulation of actin filaments and myosin-II occurs in wounds made after fixation, but before antibody incubation. Based on these considerations, we conclude that the observed pattern of cytoskeletal protein localization around the

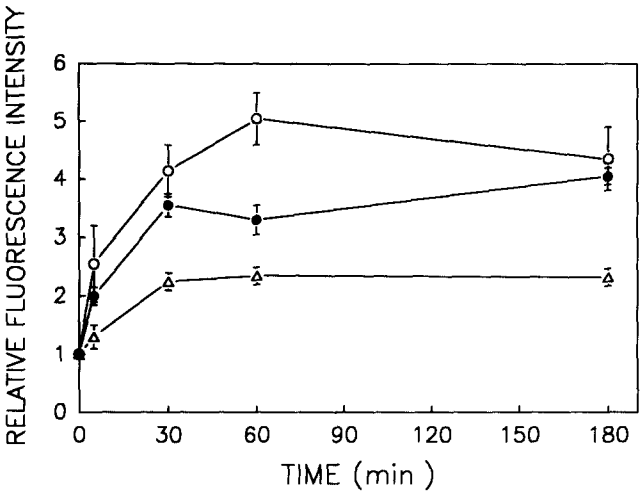


*Figure 10.* Plot of changes in relative fluorescence intensity for actin filaments (○), myosin-II (●), and ZO-1 (△) in contractile arcs and rings at wound edges at increasing time intervals following wounding. Quantification was performed as described in the Materials and Methods. For each time point, paired measurements were taken from a total of 48 cells from nine different wounds. The results are expressed as the mean ± SEM from two experiments.

wound edge is not artifactual, but instead represents a bona fide cellular response to the stimulus of wounding.

What role does this cytoskeletal structure play? The results presented in this report suggest two distinct roles, both of which have striking implications for several cell processes, including cell communication and cell polarity. The first potential role follows from the time-lapse, DIC video analysis of living, wounded cells. Namely, the cytoskeletal ring which encircles the wound in all likelihood acts to effect the observed "purse string" contraction which occurs in small wounds. This conclusion is based on: (*a*) the coincidence of arc and ring assembly with the purse string contraction; and (*b*) the fact that arcs and rings contain marked concentrations of both myosin II, a known force-producing protein, and actin filaments, the substrate upon which myosin II acts. The second potential role for the cytoskeletal ring follows from the observations that microvilli, Z0-1, and sucrase–isomaltase, which are localized at the apical domain of unwounded Caco-$2_{BBe}$ cells, remain apically localized above the ring in those cells where the ring has formed. That is, the arcs and rings may act to maintain apical/basolateral polarity along the free edges of cells which border wounds. Our results and interpretations of both wound closure and the distribution of apical proteins and structures at wound edges are somewhat heretical, so, for the sake of clarity, we will discuss each independently.

Wound repair has been the subject of numerous studies in many cell types, including gastric mucosa (Svanes et al., 1982; Rutten and Ito, 1983), intestinal epithelia (Fiel et al., 1987; Moore et al., 1989), and cultured cells derived from intestinal epithelia (McCormack et al., 1992; Nusrat et al., 1992). Results from these studies have led to the conclusion that epithelial wound repair occurs primarily as the result of lamellipodial outgrowth and cell migration into the wound as is the case in wounded fibroblast (Vasiliev, 1969) and endothelial (Odland and Ross, 1968; Krawczyk, 1971; Gabbiani et al., 1983; Wong and Gottlieb, 1988; Gordon and Staley, 1990) monolayers. That is, cells at the edge of the wound migrate into the wound area by flattening, dedifferentiating, and extending lamellipodia into the wound, similar to the fashion in which isolated fibroblasts move. In those cases where cells at the wound border remain attached to neighboring cells distal to the wound, the distal neighbors are pulled into the wound by virtue of their attachment to the migrating cell.

In the study most directly comparable to present one, wound healing was analyzed in cultured monolayers of the human intestinal epithelial cell line, T84 (Nusrat et al., 1992). In that report, it was found that large (~500-μm diam) suction wounds made in T84 monolayers healed primarily by lamellipodial extension and migration of border cells into the wound, similar to results obtained in other systems. We suspect that the differences in results found by Nusrat et al. (1992) and the present study are due primarily to the disparities in the size of the wounds. We have observed that large wounds and wounds which disrupt cell–cell contact in Caco-$2_{BBe}$ monolayers heal by cell migration, whereas smaller wounds with well-preserved cell–cell contact at wound edges heal by purse string contraction.

Why should these variations result in such a dramatic difference in cell behavior? One possibility is that assembly of the multicellular contractile ring depends on continuous (around the wound) cell–cell communication. That is, epithelial cells can somehow assess wound size and "decide" whether to assemble the contractile ring at the wound border or to dedifferentiate and migrate into the wound. Such a decision would only be useful to the epithelium if neighboring cells made the same decision—contraction of a single cell at the edge of the wound not facilitate wound closure; contraction would promote wound closure only when several cells, collectively forming an arc or ring, contract in concert. Consistent with wound-induced changes in cell–cell communication, it has been reported that cell wounding results in an increase in the number of gap junctions in cells bordering wounds (Gabbiani et al., 1978), and an increase in gap junctional communication between cells bordering wounds (Pepper et al., 1989).

Does the purse string movement of Caco-$2_{BBe}$ cells into wounds represent a wide-spread biological phenomenon or is it specific to intestinal epithelia? While the definitive answer to this question will require further study, the existing literature suggests that this mechanism is widely used for wound healing. Studies on amphibian embryos have shown that puncture wounds made in blastulae reseal by rapid, concerted movement of wound-border cells into the wound area, despite the fact that there is no cellular substrate over which the cells can migrate (Holtfreter, 1943). Similarly, scanning electron micrographs of wounds made in amphibian neurula reveal that wounds heal in the absence of lamellipodial outgrowth, in a manner consistent with the purse string–like closure described in this report (e.g., Figs. 3 and 5 in Stanisstreet et al., 1980). Moreover, two early studies of wound healing in guinea pigs concluded that the "machinery" driving would closure is localized in a tight band around the edge of the wound (Grillo et al., 1958; Watts et al., 1958). Most convincingly, a study published while the present manuscript was in preparation concluded, based on the ab-

sence of lamellipodia and the smooth appearance of wound borders, that wounded embryonic chicken epidermis heals in a purse-string fashion (Martin and Lewis, 1992). It was further suggested that this process was mediated by a cable of filamentous actin that was found to circumscribe the entire wound (Martin and Lewis, 1992). The findings of the present study provide strong, independent support for this hypothesis: not only do we document, by timelapse, DIC microscopy, a multicellular purse string contraction in living cells, we also show spatial coincidence of the actin cables with the observed purse string contraction and the colocalization of the actin cables with the actin-based mechanoenzyme, myosin-II. Our results, particularly the observation that small wounds are often cone shaped (i.e., narrow at the top and wide at the bottom), are most easily explained by a purse string contraction model of healing. Collectively, these studies provide compelling evidence that, contrary to prevailing opinion, purse string–driven cell translocation is a widely used mechanism for wound healing.

The available evidence also suggests that a similar mechanism may also be used during embryogenesis. For example, morphogenetic movements and actin filament distributions consistent with multicellular, purse string contraction are observed during tail resorption in ascidians (Cloney, 1966), as well as amphibian gastrulation (e.g., Fig. 2 in Hardin and Keller, 1988) and neurulation (Schroeder, 1970; Burnside 1971). More explicit evidence for an actomyosin-powered, purse string contraction during embryogenesis comes from studies in *Drosophila*. On the basis of cytoplasmic myosin-II localization at the edges of cell sheets undergoing invagination during dorsal closure in *Drosophila* embryos, it was proposed that such movements resulted from purse string contraction, presumably driven by myosin-II (Young et al., 1991). This hypothesis has received direct support from analysis of the *Zipper* gene (which encodes cytoplasmic myosin-II): as predicted by this hypothesis, mutations in the *Zipper* gene result in defective dorsal closure (Young et al., 1993). Based on this work in *Drosophila* (Young et al., 1991, 1993), and the apparent involvement of purse string closure mechanisms in other embryos, it seems reasonable to anticipate that multicellular actomyosin rings will play an important role in the morphogenesis of a variety of organisms.

The apparent ability of wounded cells to maintain apical localizations of microvilli, sucrase–isomaltase, and Z0-1 also runs counter to many of the current ideas about requirements for cell–cell contact for the maintenance of apical/basolateral polarity. We find that, in the presence of the specialized cytoskeletal rings which form around small wounds, at least some aspects of apical polarity are preserved, whereas in their absence, apical structures and proteins are free to move basally, even, in the case of sucrase–isomaltase, all of the way into the lamellipodia which extend onto the exposed substrate of the wound area. In other words, cells with the actomyosin arcs and rings are able to maintain a sharp boundary between apical and basolateral domains along a free edge. This finding is surprising given that a variety of studies have demonstrated a tight correlation between cell–cell contact and the maintenance of apical, basolateral polarity (for reviews see Wollner and Nelson, 1992; Rodriguez-Boulan and Powell, 1992). Indeed, disruption of cell–cell contact in MDCK epithelial cells results in the loss of polarity within 1 h (Imhof et al., 1983), and the development of cell polarity is tightly coupled to the establishment of cell–cell contact (Nelson and Veshnock, 1987; Gumbiner et al., 1988; Wang et al., 1990).

The distribution of the tight junction protein, Z0-1, is especially intriguing. Z0-1 not only remains within a single focal plane along free cell edges well above the substrate, but actually appears to be recruited specifically to the wound border. This is in clear contrast to the pattern of Z0-1 localization during Caco-2 differentiation, when Z0-1 accumulates only in areas of cell–cell contact, at the forming tight junctions (Anderson et al., 1989) and shows, in contrast to what was previously believed, cell–cell contact is not required for recruitment of Z0-1 to the cell membrane (Anderson et al., 1989; Siliciano and Goodenough, 1988). We suggest that the actomyosin rings, in conjunction with Z0-1, form a "hemijunction" which acts as a molecular corral, maintaining apical polarity even in the absence of contact with a neighboring cell. The advantages conferred upon the epithelium under these circumstances are obvious: cells able to maintain relatively normal distributions of apical proteins could, following contractile ring closure, resume normal epithelial function immediately, without the delay required by redifferentiation.

W. M. Bement is grateful to Dr. Michelle Peterson (Duke University, Durham, NC) for instruction on the handling of Caco-$2_{BBeS}$, Chi Hung Lin and Corey Thompson (Yale, New Haven, CT) for instruction in video microscopy, and members of the Mooseker laboratory for providing criticism, support, and occasionally, abuse. Thanks also to Dr. Rick Fehon (Duke University) and Dr. M. W. J. Ferguson (University of Manchester, Manchester, UK) for calling attention to several relevant studies.

This work was funded by National Institutes of Health grants GM 37756 and DK 25387 to M. S. Mooseker and MS 28695 to P. Forscher; P. Forscher was also supported by the McNight Endowment Fund for Neuroscience. W. M. Bement is a postdoctoral fellow of the American Cancer Society.

Received for publication 17 December 1992 and in revised form 8 February 1993.

### *References*

Anderson, J. M., and B. R. Stevenson. 1992. The molecular structure of the tight junction. *In* Tight Junctions. M. Cereijido, editor. 77–90.

Anderson, J. M., C. M. Van Itallie, M. D. Peterson, B. R. Stevenson, E. A. Carew, and M. S. Mooseker. 1989. Z0-1 mRNA and protein expression during tight junction assembly in Caco-2 cells. *J. Cell Biol.* 109:1047–1056.

Burnside, B. 1971. Micortubules and microfilaments in newt neurulation. *Dev. Biol.* 26:416–441.

Carboni, J. M., K. A. Conzelman, R. A. Adams, D. A. Kaiser, T. D. Pollard, and M. S. Mooseker. 1988. Structural and immunological characterization of the myosin-like 110-kD subunit of the intestinal microvillar 110K-calmodulin complex: evidence for discrete myosin head and calmodulin-binding domains. *J. Cell Biol.* 107:1749–1757.

Cloney, R. A. 1966. Cytoplasmic filaments and cell movements: epidermal cells during ascidian metamorphosis. *J. Ultrastruct. Res.* 14:300–328.

Espreafico, E. M., R. E. Cheney, M. Matteoli, A. A. C. Nascimento, P. V. De Camilli, R. E. Larson, and M. S. Mooseker. 1992. Primary structure and cellular localization of chicken myosin-V (p190), an unconventional myosin with calmodulin light chains. *J. Cell Biol.* 119:1541–1557.

Fiel, W., E. Wenzl, P. Vattay, M. Starlinger, T. Sogukoglu, and R. Schiessel. 1987. Repair of rabbit duodenal mucosa after acid injury in vivo and in vitro. *Gastroenterology.* 92:1973–1986.

Forscher, P., and S. J. Smith. 1988. Actions of cytochalasins on the organization of actin filaments and microtubules in a neuronal growth cone. *J. Cell Biol.* 107:1505–1516.

Gabbiani, G., C. Chaponnier, and I. Huttner, 1978. Cytoplasmic filaments and gap junctions in epithelial cells and myofibroblasts during wound healing. *J. Cell Biol.* 76:561–568.

Gabbiani, G., F. Gabbiani, D. Lombardi, and S. M. Schwartz. 1983. Organization of actin cytoskeleton in normal and regenerating arterial endothelial cells. *Proc. Natl. Acad. Sci. USA.* 80:2361–2364.

Gordon, S. R., and C. A. Staley. 1990. Role of the cytoskeleton during injury-

induced cell migration in corneal endothelium. *Cell Motil. Cytoskeleton.* 16:47–57.
Gordon, S. R., E. Essner, and H. Rothstein. 1982. In situ demonstration of actin in normal and injured ocular tissues using 7-nitro-2-oxa-1,3-diazole phallacidin. *Cell Motil. Cytoskeleton.* 4:343–354.
Gotlieb, A. I., L. M. May, L. Subrahmanyan, and V. I. Kalnins. 1981. Distribution of microtubule organizing centers in migrating sheets of endothelial cells. *J. Cell Biol.* 91:589–594.
Grillo, H. C., G. T. Watts, and J. Gross. 1958. Studies in wound healing: I. Contraction and the wound contents. *Ann. Surg.* 148:145–152.
Gumbiner, B., B. R. Stevenson, and A. Grimaldi. 1988. The role of the cell adhesion molecule uvomorulin in the formation and maintenance of the epithelial junctional complex. *J. Cell Biol.* 107:1575–1587.
Hardin, J., and R. Keller. 1988. The behaviour and function of bottle cells during gastrulation of *Xenopus laevis*. *Development.* 103:211–230.
Harris, A. S., J. P. Anderson, P. D. Yurechenco, L. A. D. Green, K. J. Ainger, and J. S. Morrow. 1986. Mechanisms of cytoskeletal regulation: functional and antigenic diversity in human erythrocyte and brain spectrin. *J. Cell Biochem.* 30:51–69.
Hergott, G. J., M. Sandig, and V. I. Kalnins. 1989. Cytoskeleton organization of migrating retinal pigment epithelial cells during wound healing in organ culture. *Cell Motil. Cytoskeleton.* 13:83–93.
Holtfreter, J. 1943. Properties and functions of the surface coat in amphibian embryos. *J. Exp. Zool.* 93:251–323.
Imhof, B., H. P. Vollmers, S. L. Goodman, and W. Birchmeier. 1983. Cell-cell interaction and polarity of epithelial cells: specific perturbation using a monoclonal antibody. *Cell.* 35:667–675.
Krawczyk, W. S. 1971. A pattern of epidermal cell migration during wound healing. *J. Cell Biol.* 49:247–263.
Louvard, D., M. Kedinger, and H. P. Hauri. 1992. The differentiating intestinal epithelial cell: establishment and maintenance of functions through interactions between cellular structures. *Ann. Rev. Cell Biol.* 8:157–195.
Madara, J. L. 1990. Maintenance of the macromolecular barrier at cell extrusion sites in intestinal epithelium: physiological rearrangement of tight junctions. *J. Memb. Biol.* 116:177–184.
Martin, P., and J. Lewis. 1992. Actin cables and epidermal movement in embryonic wound healing. *Nature (Lond.).* 360:179–183.
McCormack, S. A., M. J. Viar, and L. R. Johnson. 1992. Migration of IEC-6 cells: a model for mucosal healing. *Am. J. Physiol.* 263:G426–435.
Moore, R., S. Carlson, and J. L. Madara. 1989. Villus contraction aids repair of intestinal epithelium after injury. *Am. J. Physiol.* 257 (*Gastrointest. Liver Physiol. 20*). G274–G283.
Nelson, W. J., and P. J. Veshnock. 1987. Modulation of fodrin (membrane skeleton) stability by cell-cell contact in Madin-Darby canine kidney epithelial cells. *J. Cell Biol.* 104:1527–1537.
Nusrat, A., C. Delp, and J. L. Madara. 1992. Intestinal Epithelial Restitution. Characterization of a cell culture model and mapping of cytoskeletal elements in migrating cells. *J. Clin. Invest.* 89:1501–1511.
Odland, G., and R. Ross. 1968. Human wound repair I. Epidermal regeneration. *J. Cell Biol.* 39:1135–1151.
Pinto, M., S. Robine-Leon, M.-D. Appay, M. Kedinger, N. Triadou, E. Dussaulx, B. Lacroix, P. Simon-Assman, K. Haffen, J. Fogh, and A. Zweibaum. 1983. Enterocyte-like differentiation and polarization of the human colon carcinoma cell line Caco-2 in culture. *Biol. Cell* 47:323–330.
Pepper, M. S., D. C. Spray, M. Chanson, R. Montesano, L. Orci, and P. Meda. 1989. Junctional communication is induced in migrating capillary endothelial cells. *J. Cell Biol.* 109:3027–3038.
Peterson, M. D., and M. S. Mooseker. 1992. Characterization of the enterocyte-like brush border cytoskeleton of the $C2_{BBe}$ clones of the human intestinal cell line, Caco-2. *J. Cell Sci.* 102:581–600.
Quaroni, A. 1986. Crypt cell antigen expression in human tumor colonic cell lines. Analysis with a panel of monoclonal antibodies to Caco-2 luminal membrane components. *J. Natl. Cancer Inst.* 76:571–585.
Radice, G. P. 1980. The spreading of epithelial cells during wound closure in *Xenopus* larvae. *Dev. Biol.* 76:26–46.
Rodriguez-Boulan, E., and S. K. Powell. 1992. Polarity of epithelial and neuronal cells. *Ann. Rev. Cell Biol.* 8:395–427.
Rutten, M. J., and S. Ito. 1983. Morphology and electrophysiology of guinea pig gastric mucosal repair in vitro. *Am. J. Physiol.* 244 (*Gastrointest. Liver Physiol. 7*):G171–G182.
Schroeder, T. E. 1970. Neurulation in *Xenopus laevis*. An analysis and model based on light and electron microscopy. *J. Embryol. Exp. Morph.* 23:427–462.
Selden, S. C. III, and S. M. Schwartz. 1979. Cytochalasin B inhibition of endothelial proliferation at wound edges in vitro. *J. Cell Biol.* 81:348–354.
Siliciano, J. D., and D. A. Goodenough. 1988. Localization of the tight junction protein, Z0-1, is modulated by extracellular calcium and cell-cell contact in Madin-Darby canine kidney epithelial cells. *J. Cell Biol.* 107:2389–2399.
Stanisstreet, M., J. Wakely, and M. A. England. 1980. Scanning electron microscopy of wound healing in *Xenopus* and chicken embryos. *J. Embryol. Exp. Morph.* 59:341–353.
Svanes, K., S. Ito, K. Takeuchi, and W. Silen. 1982. Restitution of the surface epithelium of the in vitro frog gastric mucosa after damage with hyperosmolar sodium chloride. *Gastroenterology.* 82:1409–1426.
Takeuchi, S. 1979. Wound healing in the cornea of the chick embryo IV. Promotion of the migratory activity of isolated corneal epithelium in culture by the application of tension. *Dev. Biol.* 70:232–240.
Takeuchi, S. 1983. Wound healing in the cornea of the chick embryo V. An observation and quantitative assessment of the cell shapes in isolated corneal epithelium during spreading in vitro. *Cell Tissue Res.* 229:109–127.
Vasiliev, J. M., I. M. Gelfand, L. V. Domnina, and R. I. Rappoport. 1969. Wound healing processes in cell cultures. *Exp. Cell Res.* 54:83–93.
Wang, A. Z., G. K. Ojakian, and W. J. Nelson. 1990. Steps in the morphogenesis of a polarized epithelium. I. Uncoupling the roles of cell-cell and cell-substratum contact in establishing plasma membrane polarity in multicellular epithelial (MDCK) cysts. *J. Cell Sci.* 95:137–151.
Watts, G. T., H. C. Grillo, and J. Gross. 1958. Studies in wound healing: II. The role of the granulation tissue in contraction. *Ann. Surg.* 148:153–160.
West, A. B., C. A. Isaac, J. M. Carboni, J. S. Morrow, M. S. Mooseker, and K. W. Barwick. 1988. Localization of villin, a cytoskeletal protein specific to microvilli, in human ileum and colon and in colonic neoplasms. *Gastroenterology.* 94:343–352.
Willot, E., M. S. Balda, M. Heintzelman, B. Jameson, and J. M. Anderson. 1992. Localization and differential expression of two isoforms of the tight junction protein Z0-1. *Am. J. Phys. (Cell Physiol. 31)*:C1119–C1124.
Wollner, D. A., and W. J. Nelson. 1992. Establishing and maintaining epithelial cell polarity. Roles of protein sorting, delivery, and retention. *J. Cell Sci.* 102:85–190.
Wong, M. K. K., and A. I. Gotlieb. 1988. The reorganization of microfilaments, centrosomes, and microtubules during in vitro small wound reendothelialization. *J. Cell Biol.* 107:1777–1783.
Young, P. E., T. C. Pesacreta, and D. P. Kiehart. 1991. Dynamic changes in the distribution of cytoplasmic myosin during *Drosophila* embryogenesis. *Development.* 111:1–14.
Young, P. E., A. M. Richman, A. S. Ketchum, and D. P. Kiehart. 1993. Morphogenesis in *Drosophila* requires nonmuscle myosin heavy chain function. *Genes & Dev.* 7:29–41.